

RESEARCH ARTICLE SUMMARY

CRISPR EVOLUTION

C2c2 is a single-component programmable RNA-guided RNA-targeting CRISPR effector

Omar O. Abudayyeh, Jonathan S. Gootenberg, Silvana Konermann, Julia Joung, Ian M. Slaymaker, David B. T. Cox, Sergey Shmakov, Kira S. Makarova, Ekaterina Semenova, Leonid Minakhin, Konstantin Severinov, Aviv Regev, Eric S. Lander, Eugene V. Koonin,* Feng Zhang*

INTRODUCTION: Almost all archaea and about half of bacteria possess clustered regularly interspaced short palindromic repeat (CRISPR)–CRISPR-associated genes (Cas) adaptive immune systems, which protect microbes against viruses and other foreign DNA. All functionally characterized CRISPR systems have been reported to target DNA, with some multi-component type III systems also targeting RNA. The putative class 2 type VI system, which has not been functionally characterized, encompasses the single-effector protein C2c2, which contains two Higher Eukaryotes and Prokaryotes Nucleotide-binding (HEPN) domains commonly associated with ribonucleases (RNases), suggesting RNA-guided RNA-targeting function.

RATIONALE: Existing studies have only established a role for RNA interference, in addition to DNA interference, in the multicomponent type III-A and III-B systems. We investigated the possibility of C2c2-mediated RNA inference by heterologously expressing C2c2 locus from *Leptotrichia shahii* (LshC2c2) in the model system *Escherichia coli*. The ability of LshC2c2

to protect against MS2 single-stranded RNA (ssRNA) phage infection was assessed by using every possible spacer sequence against the phage genome. We next developed protocols to reconstitute purified recombinant LshC2c2 protein and test its biochemical activity when incubated with its mature CRISPR RNA (crRNA) and target ssRNA. We systematically evaluated the parameters necessary for cleavage. Last, to demonstrate the potential utility of the LshC2c2 complex for RNA targeting in living bacterial cells, we guided it to knockdown red fluorescent protein (RFP) mRNA in vivo.

RESULTS: This work demonstrates the RNA-guided RNase activity of the putative type VI CRISPR-effector LshC2c2. Heterologously expressed C2c2 can protect *E. coli* from MS2 phage, and by screening against the MS2 genome, we identified a H (non-G) protospacer flanking site (PFS) following the RNA target site, which was confirmed by targeting a complementary sequence in the β -lactamase transcript followed by a degenerate nucleotide sequence. Using purified LshC2c2 protein,

we demonstrate that C2c2 and crRNA are sufficient in vitro to achieve RNA-guided, PFS-dependent RNA cleavage. This cleavage preferentially occurs at uracil residues in ssRNA regions and depends on conserved catalytic residues in the two HEPN domains. Mutation

ON OUR WEBSITE

Read the full article at <http://dx.doi.org/10.1126/science.aaf5573>

of these residues yields a catalytically inactive RNA-binding protein. The secondary structure of the crRNA direct repeat (DR) stem is required for LshC2c2 activity, and mutations in the 3' region of the DR eliminate

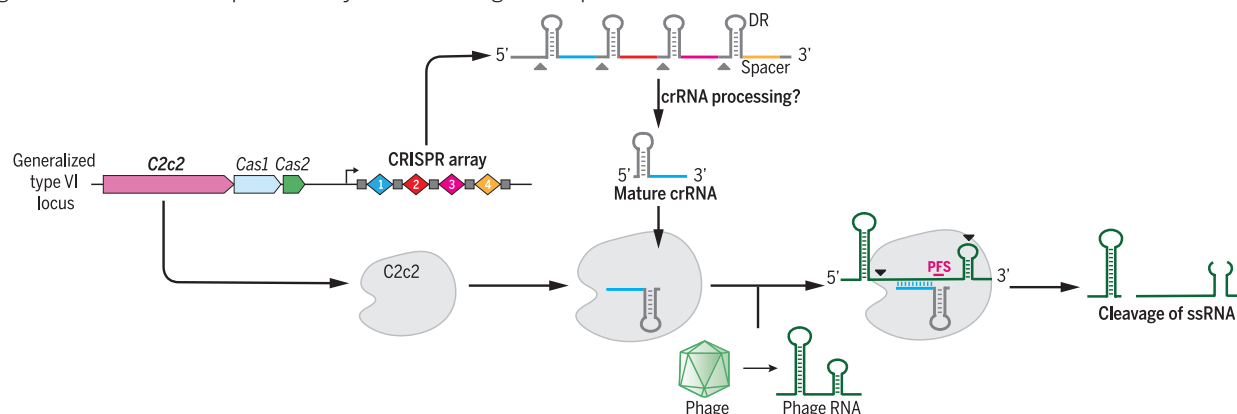
cleavage activity. Targeting is also sensitive to multiple or consecutive mismatches in the spacer:protospacer duplex. C2c2 targeting of RFP mRNA in vivo results in reduced fluorescence. The knockdown of the RFP mRNA by C2c2 slowed *E. coli* growth, and in agreement with this finding, in vitro cleavage of the target RNA results in “collateral,” nonspecific cleavage of other RNAs present in the reaction mix.

CONCLUSION: LshC2c2 is a RNA-guided RNase which requires the activity of its two HEPN domains, suggesting previously unidentified mechanisms of RNA targeting and degradation by CRISPR systems. Promiscuous RNase activity of C2c2 after activation by the target slows bacterial growth and suggests that C2c2 could protect bacteria from virus spread via programmed cell death and dormancy induction. A single-effector RNA targeting system has the potential to serve as a general chassis for molecular tools for visualizing, degrading, or binding RNA in a programmable, multiplexed fashion. ■

The list of author affiliations is available in the full article online.

*Corresponding author. Email: zhang@broadinstitute.org (F.Z.); koonin@ncbi.nlm.nih.gov (E.V.K.)
Cite this article as O. O. Abudayyeh et al., *Science* 353, aaf5573 (2016). DOI: 10.1126/science.aaf5573

C2c2 is an RNA-guided RNase that provides protection against RNA phage. CRISPR-C2c2 from *L. shahii* can be reconstituted in *E. coli* to mediate RNA-guided interference of the RNA phage MS2. Biochemical characterization of C2c2 reveals crRNA-guided RNA cleavage facilitated by the two HEPN nuclease domains. Binding of the target RNA by C2c2-crRNA also activates a nonspecific RNase activity, which may lead to promiscuous cleavage of RNAs without complementarity to the crRNA guide sequence.



RESEARCH ARTICLE

CRISPR EVOLUTION

C2c2 is a single-component programmable RNA-guided RNA-targeting CRISPR effector

Omar O. Abudayyeh,^{1,2,3,4,*} Jonathan S. Gootenberg,^{2,3,4,5,*} Silvana Konermann,^{2,3,4,*} Julia Joung,^{2,3,4} Ian M. Slaymaker,^{2,3,4} David B. T. Cox,^{1,2,3,4,6} Sergey Shmakov,^{7,8} Kira S. Makarova,⁸ Ekaterina Semenova,⁹ Leonid Minakhin,⁹ Konstantin Severinov,^{7,9,10} Aviv Regev,^{2,6} Eric S. Lander,^{2,5,6} Eugene V. Koonin,^{8,†} Feng Zhang^{1,2,3,4,†}

The clustered regularly interspaced short palindromic repeat (CRISPR)–CRISPR-associated genes (Cas) adaptive immune system defends microbes against foreign genetic elements via DNA or RNA–DNA interference. We characterize the class 2 type VI CRISPR–Cas effector C2c2 and demonstrate its RNA-guided ribonuclease function. C2c2 from the bacterium *Leptotrichia shahii* provides interference against RNA phage. In vitro biochemical analysis shows that C2c2 is guided by a single CRISPR RNA and can be programmed to cleave single-stranded RNA targets carrying complementary protospacers. In bacteria, C2c2 can be programmed to knock down specific mRNAs. Cleavage is mediated by catalytic residues in the two conserved Higher Eukaryotes and Prokaryotes Nucleotide-binding (HEPN) domains, mutations of which generate catalytically inactive RNA-binding proteins. These results broaden our understanding of CRISPR–Cas systems and suggest that C2c2 can be used to develop new RNA-targeting tools.

Almost all archaea and about half of bacteria possess clustered regularly interspaced short palindromic repeats (CRISPRs) and CRISPR-associated genes (CRISPR–Cas)–adaptive immune systems (1, 2), which protect microbes from viruses and other invading DNA through three steps: (i) adaptation—insertion of foreign nucleic acid segments (spacers) into the CRISPR array in between pairs of direct repeats (DRs); (ii) transcription and processing of the CRISPR array to produce mature CRISPR RNAs (crRNAs); and (iii) interference, by which Cas enzymes are guided by the crRNAs to target and cleave cognate sequences in the respective invader genomes (3–5). All CRISPR–Cas systems characterized to date follow these three steps, although the mechanistic implementation and proteins involved in these processes display extensive diversity.

The CRISPR–Cas systems are broadly divided into two classes on the basis of the architecture of the interference module: Class 1 systems rely on multisubunit protein complexes, whereas class 2 systems use single-effector proteins (1). Within these two classes, types and subtypes are delineated according to the presence of distinct signature genes, protein sequence conservation, and organization of the respective genomic loci. Class 1 systems include type I, in which interference is achieved through assembly of multiple Cas proteins into the Cascade complex, and type III systems, which rely on either the Csm (type III-A/D) or Cmr (Type III-B/C) effector complexes, which are distantly related to the Cascade complex (1, 6–11).

Class 2 CRISPR systems comprise type II systems, characterized by the single-component effector protein Cas9 (12–17), which contains RuvC and HNH nuclease domains, and type V systems, which use single RuvC domain-containing effectors such as Cpf1 (18), C2c1, and C2c3 (19). All functionally characterized systems, to date, have been reported to target DNA, and only the multicomponent type III-A and III-B systems additionally target RNA (7, 20–25). However, the putative class 2 type VI system is characterized by the presence of the single-effector protein C2c2, which lacks homology to any known DNA nuclease domain but contains two Higher Eukaryotes and Prokaryotes Nucleotide-binding (HEPN) domains (19). Given that all functionally characterized HEPN domains are ribonucleases (RNases) (26), there is a possibility that C2c2 functions solely as an RNA-guided RNA-targeting CRISPR effector.

HEPN domains are also found in other Cas proteins. Csm6, a component of type III-A systems, and the homologous protein Csx1, in type III-B systems, each contain a single HEPN domain and have been biochemically characterized as single-stranded RNA (ssRNA)–specific endoribonucleases (endoRNases) (21, 27, 28). In addition, type III systems contain complexes of other Cas enzymes that bind and cleave ssRNA through acidic residues associated with RNA-recognition motif (RRM) domains. These complexes (Cas10–Csm in type III-A and Cmr in type III-B) carry out RNA-guided cotranscriptional cleavage of mRNA in concert with DNA target cleavage (22, 29, 30). In contrast, the roles of Csm6 and Csx1, which cleave their targets with little specificity, are less clear, although in some cases, RNA cleavage by Csm6 apparently serves as a second line of defense when DNA-targeting fails (21). Additionally, Csm6 and Csx1 have to dimerize to form a composite active site (27, 28, 31), but C2c2 contains two HEPN domains, which suggests that it functions as a monomeric endoRNase.

As is common with class 2 systems, type VI systems are simply organized. In particular, the type VI locus in *Leptotrichia shahii* contains Cas1, Cas2, C2c2, and a CRISPR array, which is expressed and processed into mature crRNAs (19). In all CRISPR–Cas systems characterized to date, Cas1 and Cas2 are exclusively involved in spacer acquisition (32–37), which suggests that C2c2 is the sole effector protein that uses a crRNA guide to achieve interference, likely targeting RNA.

Reconstitution of the *L. shahii* C2c2 locus in *Escherichia coli* confers RNA-guided immunity

We explored whether LshC2c2 could confer immunity to MS2 (25), a lytic ssRNA phage without DNA intermediates in its life cycle that infects *E. coli*. We constructed a low-copy plasmid carrying the entire LshC2c2 locus (pLshC2c2) so as to allow for heterologous reconstitution in *E. coli* (fig. S1A). Because expressed mature crRNAs from the LshC2c2 locus have a maximum spacer length of 28 nucleotides (nt) (fig. S1A) (19), we tiled all possible 28-nt target sites in the MS2 phage genome (Fig. 1A). This resulted in a library of 3473 spacer sequences (along with 588 non-targeting guides designed to have a Levenshtein distance of ≥ 8 with respect to the MS2 and *E. coli* genomes), which we inserted between pLshC2c2 DRs. After transformation in of this construct into *E. coli*, we infected cells with varying dilutions of MS2 (10^{-1} , 10^{-3} , and 10^{-5}) and analyzed surviving cells to determine the spacer sequences carried by cells that survived the infection. Cells carrying spacers that confer robust interference against MS2 are expected to proliferate faster than those that lack such sequences. After growth for 16 hours, we identified a number of spacers that were consistently enriched across three independent infection replicates in both the 10^{-1} and 10^{-3} dilution conditions, suggesting that they enabled interference against MS2. Specifically, 152 and 144 spacers showed >0.8 log₂-fold enrichment in all three replicates for the 10^{-1} and

¹Department of Health Sciences and Technology, Massachusetts Institute of Technology, Cambridge, MA 02139, USA. ²Broad Institute of MIT and Harvard, Cambridge, MA 02142, USA.

³McGovern Institute for Brain Research at MIT, Cambridge, MA 02139, USA. ⁴Departments of Brain and Cognitive Science and Biological Engineering, Massachusetts Institute of Technology, Cambridge, MA 02139, USA. ⁵Department of Systems Biology, Harvard Medical School, Boston, MA 02115, USA. ⁶Department of Biology, Massachusetts Institute of Technology, Cambridge, MA 02139, USA. ⁷Skolkovo Institute of Science and Technology, Skolkovo, 143025, Russia. ⁸National Center for Biotechnology Information, National Library of Medicine, National Institutes of Health, Bethesda, MD 20894, USA. ⁹Waksman Institute for Microbiology, Rutgers, The State University of New Jersey, Piscataway, NJ 08854, USA. ¹⁰Institute of Molecular Genetics, Russian Academy of Sciences, Moscow, 123182, Russia.

*These authors contributed equally to this work. †Corresponding author. Email: zhang@broadinstitute.org (F.Z.); koonin@ncbi.nlm.nih.gov (E.V.K.)

10^{-3} phage dilutions, respectively; of these two groups of top enriched spacers, 75 are shared (Fig. 1B; fig. S2, A to G; and table S1). Additionally, no nontargeting guides were found to be consistently enriched among the three 10^{-1} , 10^{-3} , or 10^{-5} phage replicates (fig. S2, D and G). We also analyzed the flanking regions of protospacers on the MS2 genome corresponding to the enriched spacers and found that spacers with a G immediately flanking the 3' end of the protospacer were less fit relative to all other nucleotides at this position (A, U, or C), suggesting that the 3' protospacer-flanking site (PFS) affects the efficacy of C2c2-mediated targeting (Fig. 1C and figs. S2, E and F, and S3). Although the PFS is adjacent to the protospacer target, we chose not to use the commonly used protospacer-adjacent motif (PAM) nomenclature because it has come to connote a sequence used in self versus nonself differentiation (38), which is irrelevant in a RNA-targeting system. It is worth noting that the avoidance of G by C2c2 echoes the absence of PAMs observed for other RNA-targeting CRISPR systems and effector proteins (20, 22, 24, 25, 39, 40).

That only ~5% of crRNAs are enriched may reflect other factors influencing interference activity, such as accessibility of the target site that might be affected by RNA-binding proteins or secondary structure. In agreement with this hypothesis, the enriched spacers tend to cluster into regions of strong interference, where they are closer to each other than one would expect by random chance (fig. S3, F and G).

To validate the interference activity of the enriched spacers, we individually cloned four top-enriched spacers into pLshC2c2 CRISPR arrays and observed a 3- to 4- \log_{10} reduction in plaque formation, which is consistent with the level of enrichment observed in the screen (Fig. 1B and fig. S4). We cloned 16 guides targeting distinct regions of the MS2 *mat* gene (four guides per possible single-nucleotide PFS). All 16 crRNAs mediated MS2 interference, although higher levels of resistance were observed for the C, A, and U PFS targeting guides (Fig. 1, D and E, and fig. S5), indicating that C2c2 can be effectively retargeted in a crRNA-dependent fashion to sites within the MS2 genome.

To further validate the observed PFS preference with an alternate approach, we designed a protospacer site in the pUC19 plasmid at the 5' end of the β -lactamase mRNA, which encodes ampicillin resistance in *E. coli*, flanked by five randomized nucleotides at the 3' end. Significant depletion and enrichment was observed for the LshC2c2 locus (**** $P < 0.0001$) as compared with the pACYC184 controls (fig. S6A). Analysis of the depleted PFS sequences confirmed the presence of a PFS preference of H (fig. S6B).

C2c2 is a single-effector endoRNase mediating ssRNA cleavage with a single crRNA guide

We purified the LshC2c2 protein (fig. S7) and assayed its ability to cleave an in vitro-transcribed 173-nt ssRNA target (Fig. 2A and fig. S8) containing

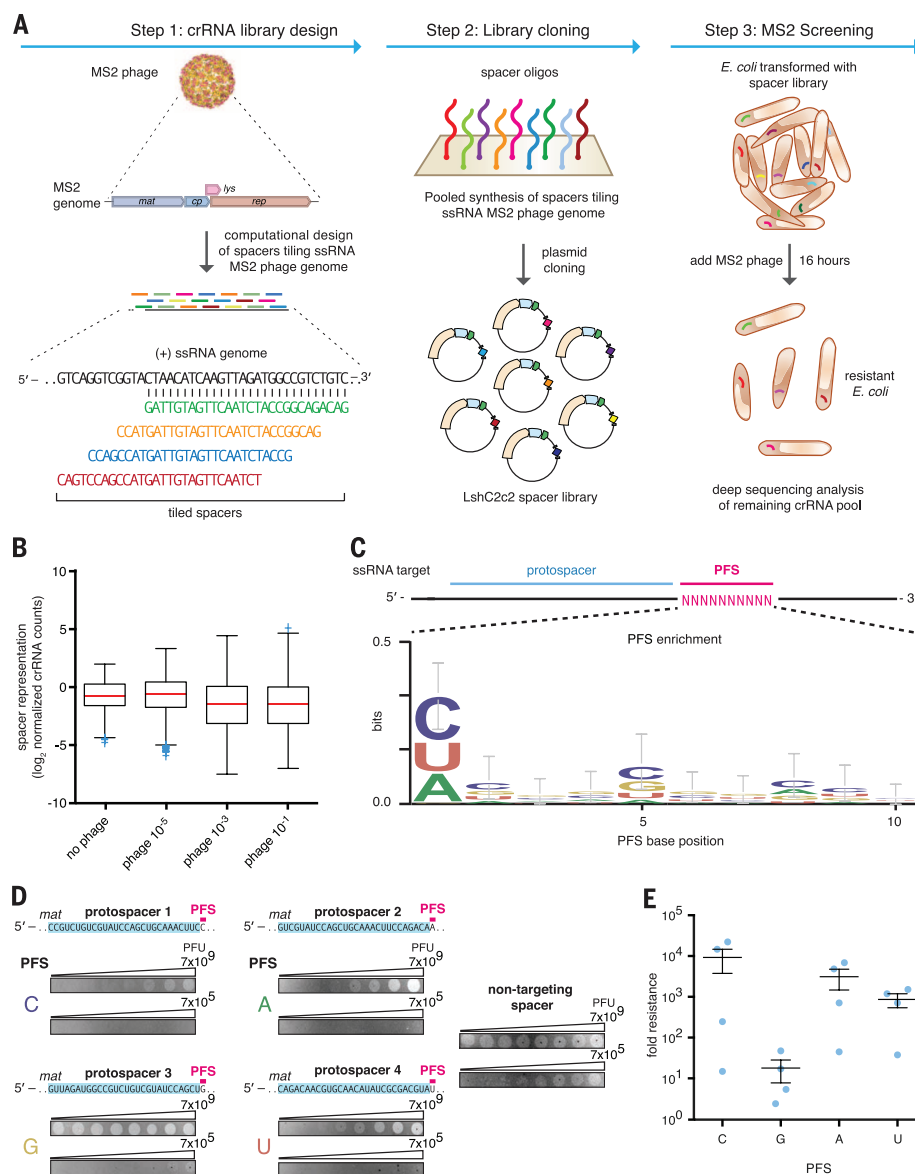


Fig. 1. Heterologous expression of the *L. shahii* C2c2 locus mediates robust interference of RNA phage in *E. coli*. (A) Schematic for the MS2 bacteriophage interference screen. A library consisting of spacers targeting all possible sequences in the MS2 RNA genome was cloned into the LshC2c2 CRISPR array. Cells transformed with the MS2-targeting spacer library were then treated with phage and plated, and surviving cells were harvested. The frequency of spacers was compared with an untreated control (no phage), and enriched spacers from the phage-treated condition were used for the generation of PFS preference logos. (B) Box plot showing the distribution of normalized crRNA frequencies for the phage-treated conditions and control screen (no phage) biological replicates ($n = 3$). The box extends from the first to third quartile, with whiskers denoting 1.5 times the interquartile range. The mean is indicated by the red horizontal bar. The 10^{-1} and 10^{-3} phage dilution distributions are significantly different than each of the control replicates [**** $P < 0.0001$ by means of analysis of variance (ANOVA) with multiple hypothesis correction]. (C) Sequence logo generated from sequences flanking the 3' end of protospacers corresponding to enriched spacers in the 10^{-3} phage dilution condition, revealing the presence of a 3' H PFS (not G). (D) Plaque assay used to validate the functional importance of the H PFS in MS2 interference. All protospacers flanked by non-G PFSs exhibited robust phage interference. Spacers were designed to target the MS2 *mat* gene, and their sequences are shown above the plaque images; the spacer used in the nontargeting control is not complementary to any sequence in either the *E. coli* or MS2 genome. Phage spots were applied as series of half-log dilutions. (E) Quantitation of MS2 plaque assay validating the H (non-G) PFS preference. Four MS2-targeting spacers were designed for each PFS. Each point on the scatter plot represents the average of three biological replicates and corresponds to a single spacer. Bars indicate the mean of four spacers for each PFS and standard error (SEM).

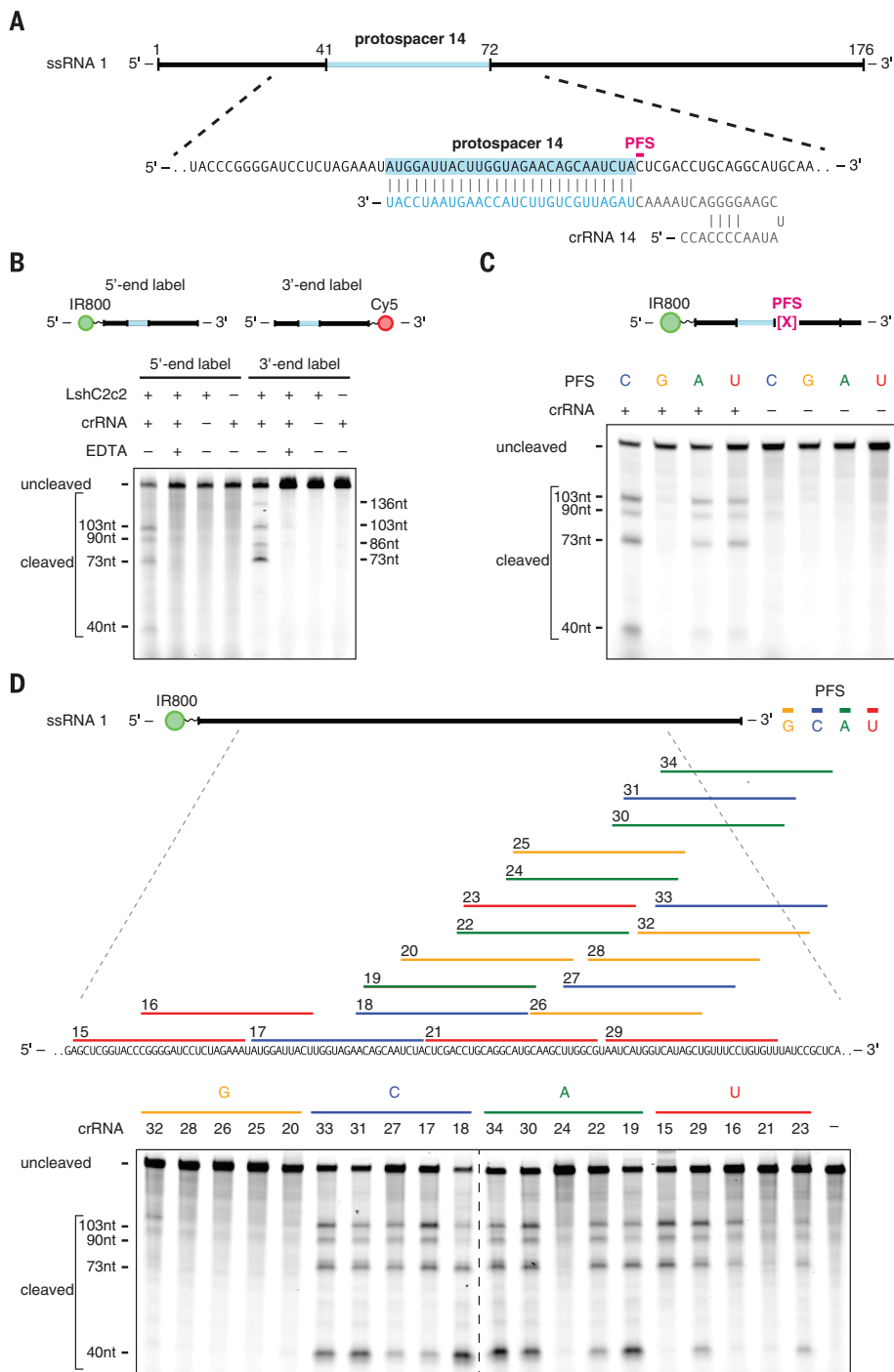


Fig. 2. LshC2c2 and crRNA mediate RNA-guided ssRNA cleavage. (A) Schematic of the ssRNA substrate being targeted by the crRNA. The protospacer region is highlighted in blue, and the PFS is indicated by the magenta bar. (B) A denaturing gel demonstrating crRNA-mediated ssRNA cleavage by LshC2c2 after 1 hour of incubation. The ssRNA target is either 5' labeled with IRDye 800 or 3' labeled with Cy5. Cleavage requires the presence of the crRNA and is abolished by addition of EDTA. Four cleavage sites are observed. Reported band lengths are matched from RNA sequencing. (C) A denaturing gel demonstrating the requirement for an H PFS (not G) after 3 hours of incubation. Four ssRNA substrates that are identical except for the PFS (indicated by the magenta "X" in the schematic) were used for the in vitro cleavage reactions. ssRNA cleavage activity is dependent on the nucleotide immediately 3' of the target site. Reported band lengths are matched from RNA sequencing. (D) Schematic showing five protospacers for each PFS on the ssRNA target (top). Denaturing gel showing crRNA-guided ssRNA cleavage activity after 1 hour of incubation. crRNAs correspond to protospacer numbering. Reported band lengths are matched from RNA sequencing.

a C PFS (ssRNA target 1 with protospacer 14). Mature LshC2c2 crRNAs contain a 28-nt DR and a 28-nt spacer (fig. S1A) (19). We therefore generated an in vitro-transcribed crRNA with a 28-nt spacer complementary to protospacer 14 on ssRNA target 1. LshC2c2 efficiently cleaved ssRNA in a Mg^{2+} - and crRNA-dependent manner (Fig. 2B and fig. S9). We then annealed complementary RNA oligos to regions flanking the crRNA target site. This partially double-stranded RNA (dsRNA) substrate was not cleaved by LshC2c2, which suggests that it is specific for ssRNA (fig. S10, A and B).

We tested the sequence constraints of RNA cleavage by LshC2c2 with additional crRNAs complementary to ssRNA target 1 in which protospacer 14 is preceded by each PFS variant. The results of this experiment confirmed the preference for C, A, and U PFSs, with little cleavage activity detected for the G PFS target (Fig. 2C). Additionally, we designed five crRNAs for each possible PFS (20 total) across the ssRNA target 1 and evaluated cleavage activity for LshC2c2 paired with each of these crRNAs. As expected, we observed less cleavage activity for G PFS-targeting crRNAs as compared with other crRNAs tested (Fig. 2D).

We then generated a dsDNA plasmid library with protospacer 14 flanked by seven random nucleotides so as to account for any PFS preference. When incubated with LshC2c2 protein and a crRNA complementary to protospacer 14, no cleavage of the dsDNA plasmid library was observed (fig. S10C). We also did not observe cleavage when targeting a ssDNA version of ssRNA target 1 from a DNA substrate. To rule out cotranscriptional DNA cleavage, which has been observed in type III CRISPR-Cas systems (22), we recapitulated the *E. coli* RNA polymerase cotranscriptional cleavage assay (fig. S11A) (22), expressing ssRNA target 1 from a DNA substrate. This assay involving purified LshC2c2 and crRNA targeting ssRNA target 1 did not show any DNA cleavage (fig. S11B). Together, these results indicate that C2c2 cleaves specific ssRNA sites directed by the target complementarity encoded in the crRNA, with a H PFS preference.

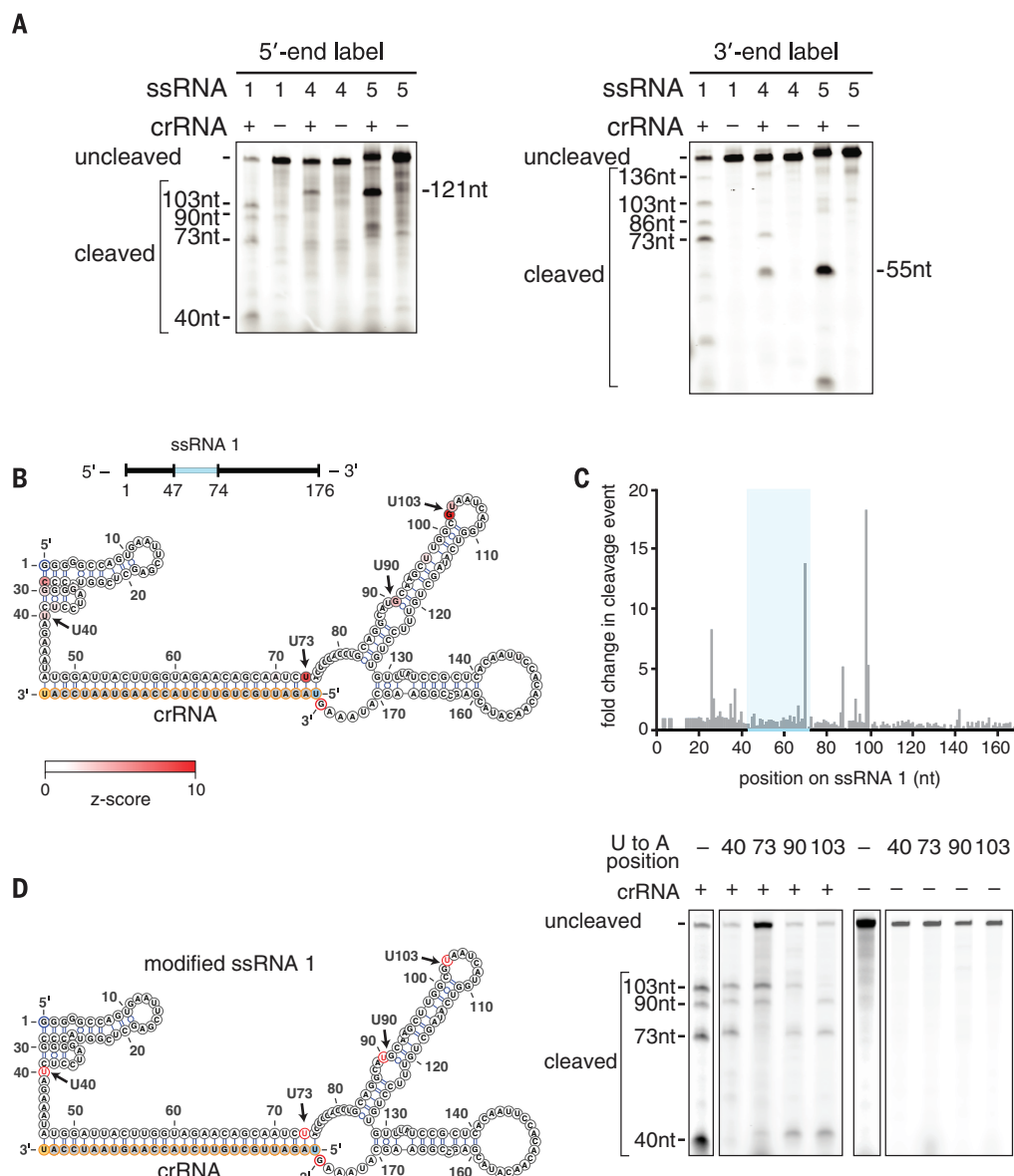
C2c2 cleavage depends on local target sequence and secondary structure

Given that C2c2 did not efficiently cleave dsRNA substrates and that ssRNA can form complex secondary structures, we reasoned that cleavage by C2c2 might be affected by secondary structure of the ssRNA target. Indeed, after tiling ssRNA target 1 from a DNA substrate. This observation suggests that the crRNA-dependent cleavage pattern was determined by features of the target sequence rather than the distance from the binding site. We hypothesized that the LshC2c2-crRNA complex binds the target and cleaves exposed regions of ssRNA within the secondary structure elements, with potential preference for certain nucleotides.

In agreement with this hypothesis, cleavage of three ssRNA targets with different sequences

Fig. 3. C2c2 cleavage sites are determined by secondary structure and sequence of the target RNA.

(A) Denaturing gel showing C2c2-crRNA-mediated cleavage after 3 hours of incubation of three nonhomopolymeric ssRNA targets (1, 4, 5; black, blue, and green, respectively, in Fig. 3, B and C, and fig. S12, A to D) that share the same protospacer but are flanked by different sequences. Despite identical protospacers, different flanking sequences resulted in different cleavage patterns. Reported band lengths are matched from RNA sequencing. **(B)** The cleavage sites of nonhomopolymer ssRNA target 1 were mapped with RNA-sequencing of the cleavage products. The frequency of cleavage at each base is colored according to the z-score and shown on the predicted crRNA-ssRNA cofold secondary structure. Fragments used to generate the frequency analysis contained the complete 5' end. The 5' and 3' end of the ssRNA target are indicated by blue and red outlines, on the ssRNA and secondary structure, respectively. The 5' and 3' end of the spacer (outlined in yellow) is indicated by the blue and orange residues highlighted, respectively. The crRNA nucleotides are highlighted in orange. **(C)** Plot of the frequencies of cleavage sites for each position of ssRNA target 1 for all reads that begin at the 5' end. The protospacer is indicated by the blue highlighted region. **(D)** Schematic of a modified ssRNA 1 target showing sites (red) of single U-to-A flips (left). Denaturing gel showing C2c2-crRNA-mediated cleavage of each of these single nucleotide variants after 3 hours of incubation (right). Reported band lengths are matched from RNA sequencing.



flanking identical 28-nt protospacers resulted in three distinct patterns of cleavage (Fig. 3A). RNA-sequencing of the cleavage products for the three targets revealed that cleavage sites mainly localized to uracil-rich regions of ssRNA or ssRNA-dsRNA junctions within the in silico-predicted cofolds of the target sequence with the crRNA (Fig. 3, B and C, and fig. S12, A to D). To test whether the LshC2c2-crRNA complex prefers cleavage at uracils, we analyzed the cleavage efficiencies of homopolymeric RNA targets (a 28-nt protospacer extended with 120 As or Us regularly interspaced by single bases of G or C to enable oligo synthesis) and found that LshC2c2 preferentially cleaved the uracil target compared with adenine (fig. S12, E and F). We then tested cleavage of a modified version of ssRNA 4 that had its main site of cleavage, a loop, replaced with each of the four possible homopolymers and found that cleavage only occurred at the uracil homopolymer loop (fig. S12G). To further test whether

cleavage was occurring at uracil residues, we mutated single-uracil residues in ssRNA 1 that showed cleavage in the RNA-sequencing (Fig. 3B) to adenines. This experiment showed that by mutating each uracil residue, we could modulate the presence of a single cleavage band, which is consistent with LshC2c2 cleaving at uracil residues in ssRNA regions (Fig. 3D).

The HEPN domains of C2c2 mediate RNA-guided ssRNA-cleavage

Bioinformatic analysis of C2c2 has suggested that the HEPN domains are likely to be responsible for the observed catalytic activity (19). Each of the two HEPN domains of C2c2 contains a dyad of conserved arginine and histidine residues (Fig. 4A), which is in agreement with the catalytic mechanism of the HEPN endoRNase (26–28). We mutated each of these putative catalytic residues separately to alanine (R597A, H602A, R1278A, H1283A) in the LshC2c2 locus

plasmids and assayed for MS2 interference. None of the four mutant plasmids were able to protect *E. coli* from phage infection (Fig. 4B and fig. S13). (Single-letter abbreviations for the amino acid residues are as follows: A, Ala; C, Cys; D, Asp; E, Glu; F, Phe; G, Gly; H, His; I, Ile; K, Lys; L, Leu; M, Met; N, Asn; P, Pro; Q, Gln; R, Arg; S, Ser; T, Thr; V, Val; W, Trp; and Y, Tyr. In the mutants, other amino acids were substituted at certain locations; for example, R597A indicates that arginine at position 597 was replaced by alanine.)

We purified the four single-point mutant proteins and assayed their ability to cleave 5' end-labeled ssRNA target 1 (Fig. 4C). In agreement with our in vivo results, all four mutations abolished cleavage activity. The inability of either of the two wild-type HEPN domains to compensate for inactivation of the other implies cooperation between the two domains. These results agree with observations that several bacterial and eukaryotic single-HEPN proteins function as dimers (27, 28, 41).

Catalytically inactive variants of Cas9 retain target DNA binding, allowing for the creation of programmable DNA-binding proteins (12, 13). Electrophoretic mobility shift assays (EMSAs) on both the wild-type (Fig. 4D) and R1278A mutant LshC2c2 (Fig. 4E) in complex with crRNA showed the wild-type LshC2c2 complex binding strongly [dissociation constant (K_d) ~ 46 nM] (fig. S14A) and specifically to 5' end-labeled ssRNA target 10 but not to the 5' end-labeled nontarget ssRNA (the reverse complement of ssRNA target 10). The R1278A mutant C2c2 complex showed even stronger (K_d ~ 7 nM) (fig. S14B) specific binding, indicating that this HEPN mutation results in a catalytically inactive, RNA-programmable, RNA-binding protein. The LshC2c2 protein or crRNA alone showed reduced levels of target affinity, as expected (fig. S14, C to E). Additionally, no specific binding of LshC2c2-crRNA complex to ssDNA was observed (fig. S15).

These results demonstrate that C2c2 cleaves RNA via a catalytic mechanism distinct from other known CRISPR-associated RNases. In particular, the type III Csm and Cmr multiprotein complexes rely on acidic residues of RRM domains for catalysis, whereas C2c2 achieves RNA cleavage through the conserved basic residues of its two HEPN domains.

Sequence and structural requirements of C2c2 crRNA

Similar to the type V-A (Cpf1) systems (18), the LshC2c2 crRNA contains a single stem loop in the DR, suggesting that the secondary structure of the crRNA could facilitate interaction with LshC2c2. We thus investigated the length requirements of the spacer sequence for ssRNA cleavage and found that LshC2c2 requires spacers of at least 22 nt length to efficiently cleave ssRNA target 1 (fig. S16A). The stem-loop structure of the crRNA is also critical for ssRNA cleavage because DR truncations that disturbed the stem loop abrogated target cleavage (fig. S16B). Thus, a DR longer than 24 nt is required to maintain the stem loop necessary for LshC2c2 to mediate ssRNA cleavage.

Single-base-pair inversions in the stem that preserved the stem structure did not affect the activity of the LshC2c2 complex. In contrast, inverting all four G-C pairs in the stem eliminated the cleavage, despite maintaining the duplex structure (fig. S17A). Other perturbations, such as those that introduced kinks and reduced or increased base-pairing in the stem, also eliminated or drastically suppressed cleavage. This suggests that the crRNA stem length is important for complex formation and activity (fig. S17A). We also found that loop deletions eliminated cleavage, whereas insertions and substitutions mostly maintained some level of cleavage activity (fig. S17B). In contrast, nearly all substitutions or deletions in the region 3' to the DR prevented cleavage by LshC2c2 (fig. S18). Together, these results demonstrate that LshC2c2 recognizes structural characteristics of its cognate crRNA but is amenable to loop insertions and most tested base substitutions outside of the 3' DR region.

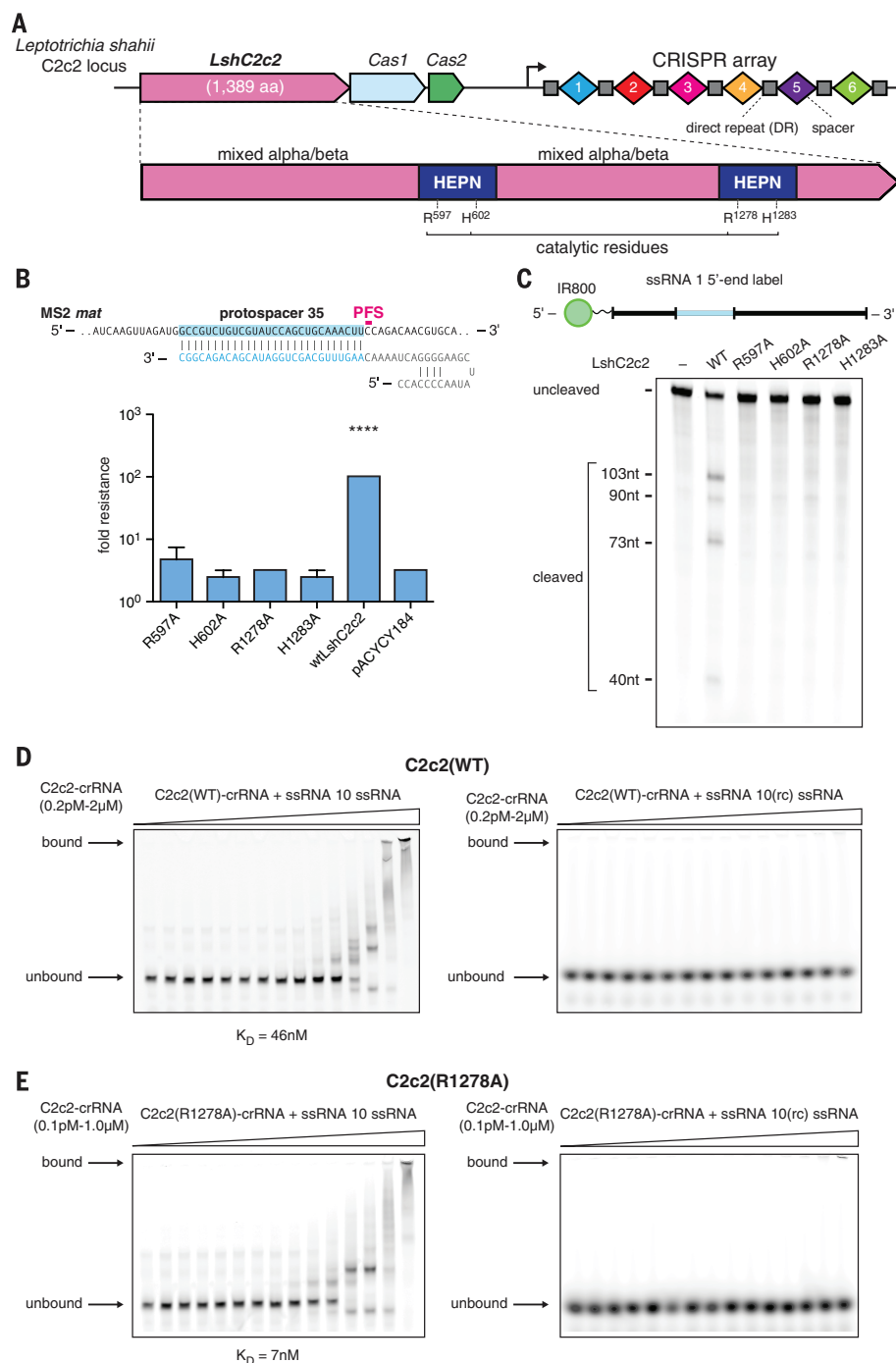
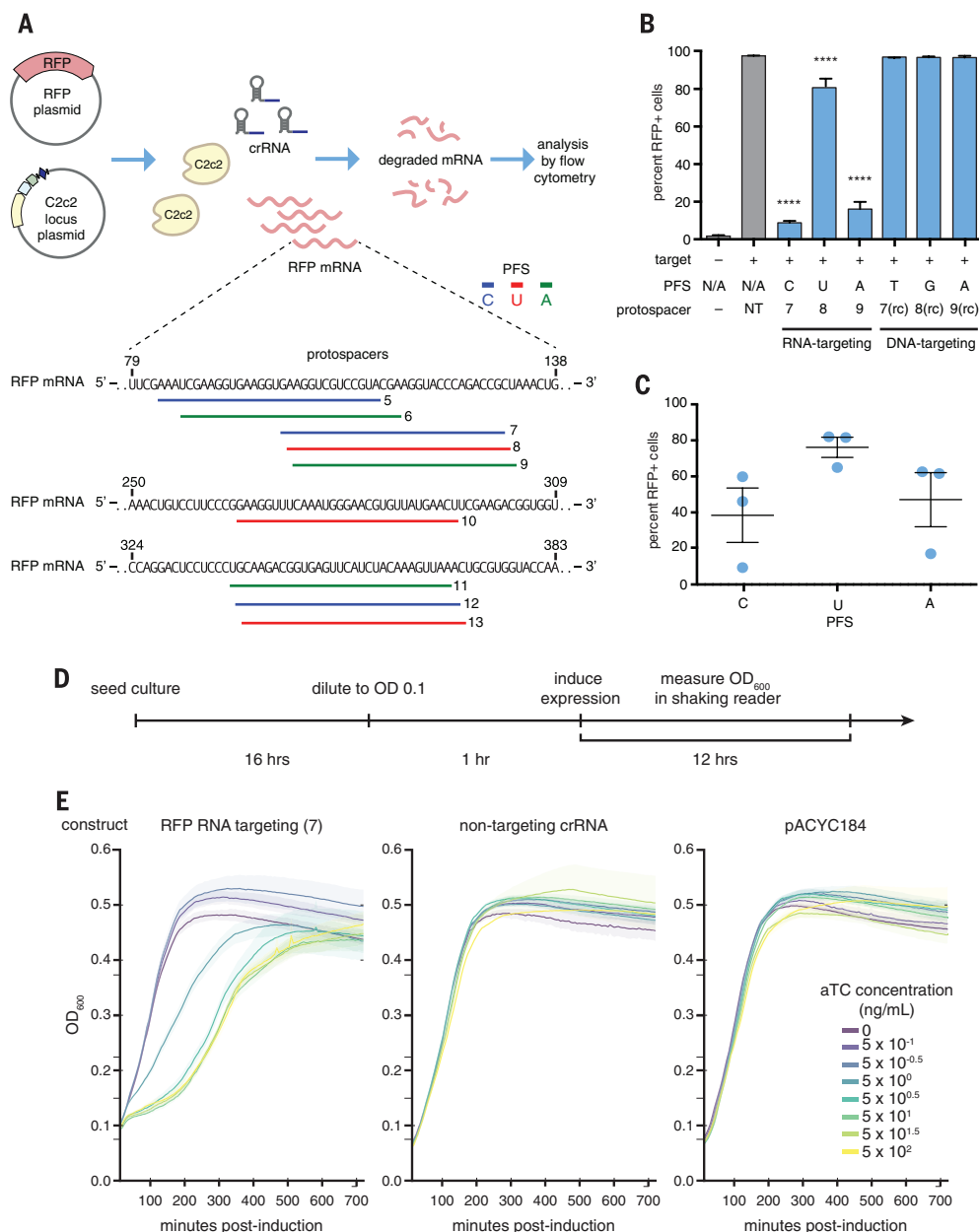


Fig. 4. The two HEPN domains of C2c2 are necessary for crRNA-guided ssRNA cleavage but not for binding. (A) Schematic of the *LshC2c2* locus and the domain organization of the LshC2c2 protein, showing conserved residues in HEPN domains (dark blue). (B) Quantification of MS2 plaque assay with HEPN catalytic residue mutants. For each mutant, the same crRNA targeting protospacer 35 was used. ($n = 3$ biological replicates, **** $P < 0.0001$ compared with pACYC184 by Student's t test. Bars represent mean \pm SEM). (C) Denaturing gel showing conserved residues of the HEPN motif, indicated as catalytic residues in (A), are necessary for crRNA-guided ssRNA target 1 cleavage after 3 hours of incubation. Reported band lengths are matched from RNA sequencing. (D) Electrophoretic mobility shift assay (EMSA) evaluating affinity of the wild-type LshC2c2-crRNA complex against a targeted (left) and a nontargeted (right) ssRNA substrate. The nontargeted ssRNA substrate is the reverse complement of the targeted ssRNA 10. EDTA is supplemented to reaction condition in order to reduce any cleavage activity. (E) Electrophoretic mobility shift assay with LshC2c2(R1278A)-crRNA complex against on-target ssRNA 10 and nontargeting ssRNA [same substrate sequences as in (D)].

Fig. 5. RFP mRNA knockdown by retargeting LshC2c2. (A) Schematic showing crRNA-guided knockdown of RFP in *E. coli* heterologously expressing the LshC2c2 locus. Three RFP-targeting spacers were selected for each non-G PFS, and each protospacer on the RFP mRNA is numbered. (B) RFP mRNA-targeting spacers effected RFP knockdown, whereas DNA-targeting spacers (targeting the noncoding strand of the RFP gene on the expression plasmid, indicated as “rc” spacers) did not affect RFP expression. (*n* = 3 biological replicates, *****P* < 0.0001 compared with nontargeting guide by means of ANOVA with multiple hypothesis correction. Bars represent mean ± SEM). (C) Quantification of RFP knockdown in *E. coli*. Three spacers each targeting C, U, or A PFS-flanking protospacers [nine spacers, numbered 5 to 13 as indicated in (A)] in the RFP mRNA were introduced, and RFP expression was measured with flow cytometry. Each point on the scatter plot represents the average of three biological replicates and corresponds to a single spacer. Bars indicate the mean of three spacers for each PFS, and errors bars are shown as the SEM. (D) Timeline of *E. coli* growth assay. (E) Effect of RFP mRNA targeting on the growth rate of *E. coli* transformed with an inducible RFP expression plasmid as well as the LshC2c2 locus with nontargeting, RNA targeting (spacer complementary to the RFP mRNA or RFP gene coding strand), and pACYC control plasmid at different anhydrotetracycline (aTC) concentrations.



These results have implications for the future application of C2c2-based tools that require guide engineering for recruitment of effectors or modulation of activity (42–44).

C2c2 cleavage is sensitive to double mismatches in the crRNA-target duplex

We tested the sensitivity of the LshC2c2 system to single mismatches between the crRNA guide and target RNA by mutating single bases across the spacer to the respective complementary bases (for example, A to U). We then quantified plaque formation with these mismatched spacers in the MS2 infection assay and found that C2c2 was fully tolerant to single mismatches across the spacer because such mismatched spacers interfered with phage propagation with similar efficiency as fully matched spacers (figs. S19A and S20). However,

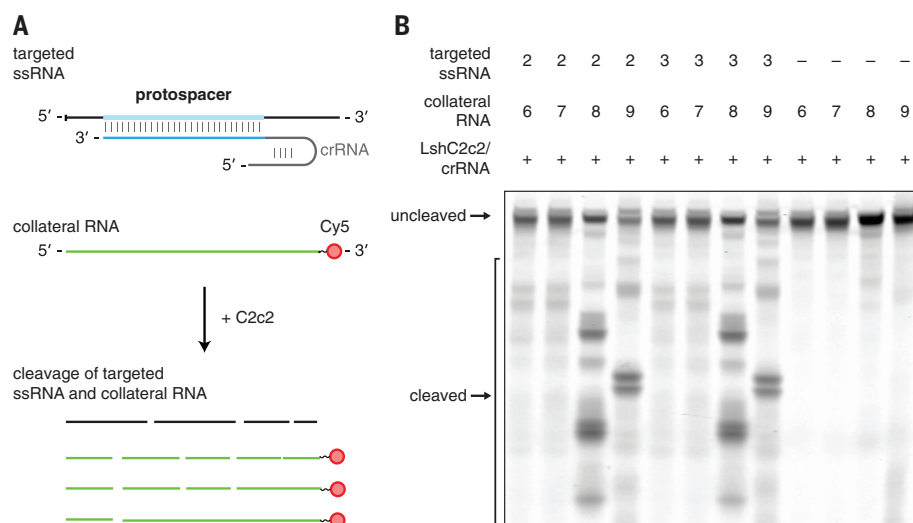
when we introduced consecutive double substitutions in the spacer, we found a ~3-log₁₀-fold reduction in the protection for mismatches in the center, but not at the 5' or 3' end, of the crRNA (figs. S19B and S20). This observation suggests the presence of a mismatch-sensitive “seed region” in the center of the crRNA-target duplex.

We generated a set of in vitro-transcribed crRNAs with mismatches similarly positioned across the spacer region. When incubated with LshC2c2 protein, all single mismatched crRNA supported cleavage (fig. S19C), which is in agreement with our in vivo findings. When tested with a set of consecutive and nonconsecutive double-mutant crRNAs, LshC2c2 was unable to cleave the target RNA if the mismatches were positioned in the center, but not at the 5' or 3' end of the crRNA (figs. S19D and S21A), further sup-

porting the existence of a central seed region. Additionally, no cleavage activity was observed with crRNAs containing consecutive triple mismatches in the seed region (fig. S21B).

C2c2 can be reprogrammed to mediate specific mRNA knockdown in vivo

Given the ability of C2c2 to cleave target ssRNA in a crRNA sequence-specific manner, we tested whether LshC2c2 could be reprogrammed to degrade selected nonphage ssRNA targets, and particularly mRNAs, in vivo. We cotransformed *E. coli* with a plasmid encoding LshC2c2 and a crRNA targeting the mRNA of red fluorescent protein (RFP) as well as a compatible plasmid expressing RFP (Fig. 5A). For optical density (OD)-matched samples, we observed an ~20 to 92% decrease in RFP-positive cells for crRNAs



targeting protospacers flanked by C, A, or U PFSs (Fig. 5, B and C). As a control, we tested crRNAs containing reverse complements (targeting the dsDNA plasmid) of the top performing RFP mRNA-targeting spacers. As expected, we observed no decrease in RFP fluorescence by these crRNAs (Fig. 5B). We also confirmed that mutation of the catalytic arginine residues in either HEPN domain to alanine precluded RFP knock-down (fig. S22). Thus, C2c2 is capable of general retargeting to arbitrary ssRNA substrates, governed exclusively by predictable nucleic-acid interactions.

When we examined the growth of cells carrying the RFP-targeting spacer with the greatest level of RFP knockdown, we noted that the growth rate of these bacteria was substantially reduced (Fig. 5A, spacer 7). We investigated whether the effect on growth was mediated by the RFP mRNA-targeting activity of LshC2c2 by introducing an inducible-RFP plasmid and an RFP-targeting LshC2c2 locus into *E. coli*. Upon induction of RFP transcription, cells with RFP knockdown showed substantial growth suppression not observed in nontargeting controls (Fig. 5, D and E). This growth restriction was dependent on the level of the RFP mRNA, as controlled by the concentration of the inducer anhydrotetracycline. In contrast, in the absence of RFP transcription, we did not observe any growth restriction, nor did we observe any transcription-dependent DNA-targeting in our biochemical experiment (fig. S11). These results indicate that RNA-targeting is likely the primary driver of this growth restriction phenotype. We therefore surmised that in addition to the cleavage of the target RNA,

C2c2 CRISPR systems might prevent virus reproduction also via nonspecific cleavage of cellular mRNAs, causing programmed cell death (PCD) or dormancy (45, 46).

C2c2 cleaves collateral RNA in addition to crRNA-targeted ssRNA

Cas9 and Cpf1 cleave DNA within the crRNA-target heteroduplex at defined positions, reverting to an inactive state after cleavage. In contrast, C2c2 cleaves the target RNA outside of the crRNA binding site at varying distances depending on the flanking sequence, presumably within exposed ssRNA loop regions (Fig. 3, B and C, and fig. S12, A to D). This observed flexibility with respect to the cleavage distance led us to test whether cleavage of other, non-target ssRNAs also occurs upon C2c2 target-binding and activation. Under this model, the C2c2-crRNA complex, once activated by binding to its target RNA, cleaves the target RNA as well as other RNAs nonspecifically. We carried out *in vitro* cleavage reactions that included, in addition to LshC2c2 protein, crRNA and its target RNA, one of four unrelated RNA molecules without any complementarity to the crRNA guide (Fig. 6A). These experiments showed that whereas the LshC2c2-crRNA complex did not mediate cleavage of any of the four collateral RNAs in the absence of the target RNA, all four were efficiently degraded in the presence of the target RNA (Fig. 6B and fig. S23A). Furthermore, R597A and R1278A HEPN mutants were unable to cleave collateral RNA (fig. S23B).

To further investigate the collateral cleavage and growth restriction *in vivo*, we hypothesized

that if a PFS preference screen for LshC2c2 was performed in a transcribed region on the transformed plasmid, then we should be able to detect the PFS preference due to growth restriction induced by RNA-targeting. We designed a protospacer site flanked by five randomized nucleotides at the 3' end in either a nontranscribed region or in a region transcribed from the *lac* promoter (fig. S24A). The analysis of the depleted and enriched PFS sequences identified a H PFS only in the assay with the transcribed sequence but no discernable motif in the nontranscribed sequence (fig. S24, B and C).

These results suggest a HEPN-dependent mechanism by which C2c2 in a complex with crRNA is activated upon binding to target RNA and subsequently cleaves nonspecifically other available ssRNA targets. Such promiscuous RNA cleavage could cause cellular toxicity, resulting in the observed growth rate inhibition. These findings imply that in addition to their likely role in direct suppression of RNA viruses, type VI CRISPR-Cas systems could function as mediators of a distinct variety of PCD or dormancy induction that is specifically triggered by cognate invader genomes (Fig. 7). Under this scenario, dormancy would slow the infection and supply additional time for adaptive immunity. Such a mechanism agrees with the previously proposed coupling of adaptive immunity and PCD during the CRISPR-Cas defensive response (47).

Conclusions

The class 2 type VI effector protein C2c2 is a RNA-guided RNase that can be efficiently programmed to degrade any ssRNA by specifying a 28-nt sequence on the crRNA (fig. S10). C2c2 cleaves RNA through conserved basic residues within its two HEPN domains, in contrast to the catalytic mechanisms of other known RNases found in CRISPR-Cas systems (25, 48). Alanine substitution of any of the four predicted HEPN domain catalytic residues converted C2c2 into an inactive programmable RNA-binding protein (dC2c2, analogous to dCas9). Many different spacer sequences work well in our assays, although further screening will likely define properties and rules governing optimal function.

These results suggest a broad range of biotechnology applications and research questions (49–51). For example, the ability of dC2c2 to bind to specified sequences could be used to (i) bring effector modules to specific transcripts in order to modulate their function or translation, which could be used for large-scale screening, construction of synthetic regulatory circuits, and other purposes; (ii) fluorescently tag specific RNAs in order to visualize their trafficking and/or localization; (iii) alter RNA localization through domains with affinity for specific subcellular compartments; and (iv) capture specific transcripts (through direct pull-down of dC2c2) in order to enrich for proximal molecular partners, including RNAs and proteins.

Active C2c2 also has many potential applications, such as targeting a specific transcript for destruction, as performed here with RFP.

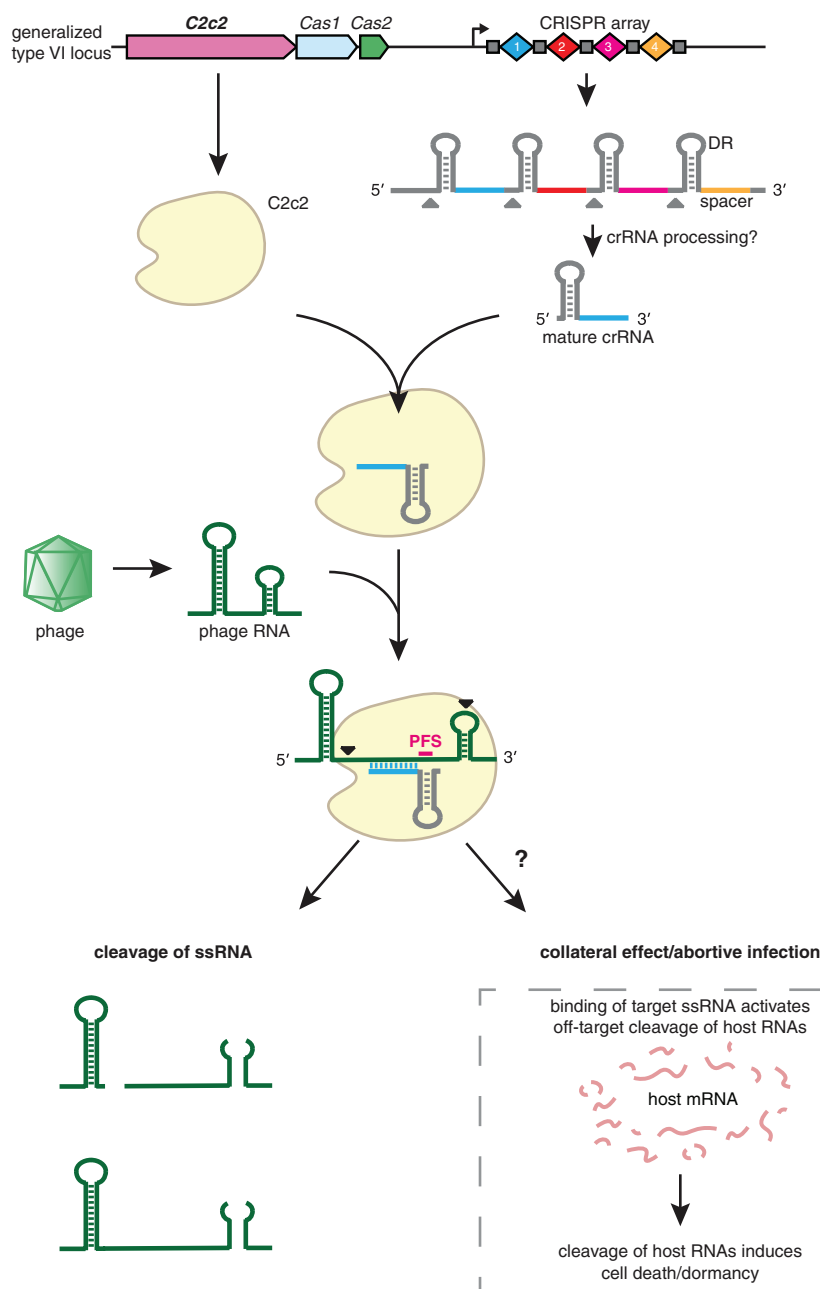


Fig. 7. C2c2 as a putative RNA-targeting prokaryotic immune system. The C2c2-crRNA complex recognizes target RNA via base pairing with the cognate protospacer and cleaves the target RNA. In addition, binding of the target RNA by C2c2-crRNA activates a nonspecific RNase activity, which may lead to promiscuous cleavage of RNAs without complementarity to the crRNA guide sequence. Through this nonspecific RNase activity, C2c2 may also cause abortive infection via programmed cell death or dormancy induction.

In addition, C2c2, once primed by the cognate target, can cleave other (noncomplementary) RNA molecules *in vitro* and inhibit cell growth *in vivo*. Biologically, this promiscuous RNase activity might reflect a PCD/dormancy-based protection mechanism of the type VI CRISPR-Cas systems (Fig. 7). Technologically, it might be used to trigger PCD or dormancy in specific cells, such as cancer cells expressing a particular transcript, neurons of a given class, or cells infected by a specific pathogen.

Further experimental study is required to elucidate the mechanisms by which the C2c2 system acquires spacers and the classes of pathogens against which it protects bacteria. The presence of the conserved CRISPR adaptation module consisting of typical Cas1 and Cas2 proteins in the LshC2c2 locus suggests that it is capable of spacer acquisition. Although C2c2 systems lack reverse transcriptases, which mediate acquisition of RNA spacers in some type III systems (52), it is possible that additional host or

viral factors could support RNA spacer acquisition. Additionally or alternatively, type VI systems could acquire DNA spacers similar to other CRISPR-Cas variants but then target transcripts of the respective DNA genomes, eliciting PCD and abortive infection (Fig. 7).

The CRISPR-C2c2 system represents a distinct evolutionary path among class 2 CRISPR-Cas systems. It is likely that other, broadly analogous class 2 RNA-targeting immune systems exist, and further characterization of the diverse members of class 2 systems will provide a deeper understanding of bacterial immunity and provide a rich starting point for the development of programmable molecular tools for *in vivo* RNA manipulation.

Materials and methods

Expanded materials and methods, including computational analysis, can be found in supplementary materials and methods.

Bacterial phage interference

The C2c2 CRISPR locus was amplified from DNA from *Leptotrichia shahii* DSM 19757 (ATCC, Manassas, VA) and cloned for heterologous expression in *E. coli*. For screens, a library of all possible spacers targeting the MS2 genome were cloned into the spacer array; for individual spacers, single specific spacers were cloned into the array. Interference screens were performed in liquid culture and plated; surviving colonies were harvested for DNA and spacer representation was determined by next-generation sequencing. Individual spacers were tested by spotting on top agar.

β -lactamase and transcribed/non-transcribed PFS preference screens

Sequences with randomized nucleotides adjacent to protospacer 1 were cloned into pUC19 in corresponding regions. Libraries were screened by co-transformation with LshC2c2 locus plasmid or pACYC184 plasmid control, harvesting of the surviving colonies, and next-generation sequencing of the resulting regions.

RFP-targeting assay

Cells containing an RFP expressing plasmid were transformed with an LshC2c2 locus plasmid with corresponding spacers, grown overnight, and analyzed for RFP fluorescence by flow cytometry. The growth effects of LshC2c2 activity were quantified by titrating inducible RFP levels with dilutions of anhydrotetracycline inducer and then measuring OD₆₀₀.

in vitro nuclease and electrophoretic mobility shift assays

LshC2c2 protein and HEPN mutants were purified for use in *in vitro* reactions; RNA were synthesized *in vitro* transcription. For nuclease assays, protein was co-incubated with crRNA and either 3' or 5'-labeled targets and analyzed via denaturing gel electrophoresis and imaging or by next-generation sequencing. For electrophoretic mobility shift assays, protein and nucleic

acid were co-incubated and then resolved by gel electrophoresis and imaging.

REFERENCES AND NOTES

- K. S. Makarova *et al.*, An updated evolutionary classification of CRISPR-Cas systems. *Nat. Rev. Microbiol.* **13**, 722–736 (2015). doi: [10.1038/nrmicro3569](https://doi.org/10.1038/nrmicro3569); pmid: [26411297](https://pubmed.ncbi.nlm.nih.gov/26411297/)
- K. S. Makarova *et al.*, Evolution and classification of the CRISPR-Cas systems. *Nat. Rev. Microbiol.* **9**, 467–477 (2011). doi: [10.1038/nrmicro2577](https://doi.org/10.1038/nrmicro2577); pmid: [21552286](https://pubmed.ncbi.nlm.nih.gov/21552286/)
- A. V. Wright, J. K. Nuñez, J. A. Doudna, Biology and applications of CRISPR systems: Harnessing nature's toolbox for genome engineering. *Cell* **164**, 29–44 (2016). doi: [10.1016/j.cell.2015.12.035](https://doi.org/10.1016/j.cell.2015.12.035); pmid: [26771484](https://pubmed.ncbi.nlm.nih.gov/26771484/)
- L. A. Marraffini, CRISPR-Cas immunity in prokaryotes. *Nature* **526**, 55–61 (2015). doi: [10.1038/nature15386](https://doi.org/10.1038/nature15386); pmid: [26432244](https://pubmed.ncbi.nlm.nih.gov/26432244/)
- J. van der Oost, M. M. Jore, E. R. Westra, M. Lundgren, S. J. Brouns, CRISPR-based adaptive and heritable immunity in prokaryotes. *Trends Biochem. Sci.* **34**, 401–407 (2009). doi: [10.1016/j.tibs.2009.05.002](https://doi.org/10.1016/j.tibs.2009.05.002); pmid: [19945378](https://pubmed.ncbi.nlm.nih.gov/19945378/)
- S. J. Brouns *et al.*, Small CRISPR RNAs guide antiviral defense in prokaryotes. *Science* **321**, 960–964 (2008). doi: [10.1126/science.1159689](https://doi.org/10.1126/science.1159689); pmid: [18703739](https://pubmed.ncbi.nlm.nih.gov/18703739/)
- C. R. Hale *et al.*, RNA-guided RNA cleavage by a CRISPR RNA-Cas protein complex. *Cell* **139**, 945–956 (2009). doi: [10.1016/j.cell.2009.07.040](https://doi.org/10.1016/j.cell.2009.07.040); pmid: [19945378](https://pubmed.ncbi.nlm.nih.gov/19945378/)
- R. N. Jackson *et al.*, Crystal structure of the CRISPR RNA-guided surveillance complex from *Escherichia coli*. *Science* **345**, 1473–1479 (2014). doi: [10.1126/science.1256328](https://doi.org/10.1126/science.1256328); pmid: [25103409](https://pubmed.ncbi.nlm.nih.gov/25103409/)
- L. A. Marraffini, E. J. Sontheimer, CRISPR interference limits horizontal gene transfer in staphylococci by targeting DNA. *Science* **322**, 1843–1845 (2008). doi: [10.1126/science.1165771](https://doi.org/10.1126/science.1165771); pmid: [19095942](https://pubmed.ncbi.nlm.nih.gov/19095942/)
- S. Mulepati, A. Héroux, S. Bailey, Crystal structure of a CRISPR RNA-guided surveillance complex bound to a ssDNA target. *Science* **345**, 1479–1484 (2014). doi: [10.1126/science.1256996](https://doi.org/10.1126/science.1256996); pmid: [25123481](https://pubmed.ncbi.nlm.nih.gov/25123481/)
- T. Sinkunas *et al.*, In vitro reconstitution of Cascade-mediated CRISPR immunity in *Streptococcus thermophilus*. *EMBO J.* **32**, 385–394 (2013). doi: [10.1038/emboj.2012.352](https://doi.org/10.1038/emboj.2012.352); pmid: [23334296](https://pubmed.ncbi.nlm.nih.gov/23334296/)
- G. Gasinunas, R. Barrangou, P. Horvath, V. Siksnys, Cas9-crRNA ribonucleoprotein complex mediates specific DNA cleavage for adaptive immunity in bacteria. *Proc. Natl. Acad. Sci. U.S.A.* **109**, E2579–E2586 (2012). doi: [10.1073/pnas.1208507109](https://doi.org/10.1073/pnas.1208507109); pmid: [22949671](https://pubmed.ncbi.nlm.nih.gov/22949671/)
- M. Jinek *et al.*, A programmable dual-RNA-guided DNA endonuclease in adaptive bacterial immunity. *Science* **337**, 816–821 (2012). doi: [10.1126/science.1225829](https://doi.org/10.1126/science.1225829); pmid: [22745249](https://pubmed.ncbi.nlm.nih.gov/22745249/)
- E. Deltcheva *et al.*, CRISPR RNA maturation by trans-encoded small RNA and host factor RNase III. *Nature* **471**, 602–607 (2011). doi: [10.1038/nature09886](https://doi.org/10.1038/nature09886); pmid: [21455174](https://pubmed.ncbi.nlm.nih.gov/21455174/)
- R. Sapranaukas *et al.*, The *Streptococcus thermophilus* CRISPR/Cas system provides immunity in *Escherichia coli*. *Nucleic Acids Res.* **39**, 9275–9282 (2011). doi: [10.1093/nar/gkr606](https://doi.org/10.1093/nar/gkr606); pmid: [21813460](https://pubmed.ncbi.nlm.nih.gov/21813460/)
- J. E. Garneau *et al.*, The CRISPR/Cas bacterial immune system cleaves bacteriophage and plasmid DNA. *Nature* **468**, 67–71 (2010). doi: [10.1038/nature09523](https://doi.org/10.1038/nature09523); pmid: [21048762](https://pubmed.ncbi.nlm.nih.gov/21048762/)
- R. Barrangou *et al.*, CRISPR provides acquired resistance against viruses in prokaryotes. *Science* **315**, 1709–1712 (2007). doi: [10.1126/science.1138140](https://doi.org/10.1126/science.1138140); pmid: [17379808](https://pubmed.ncbi.nlm.nih.gov/17379808/)
- B. Zetsche *et al.*, Cpf1 is a single RNA-guided endonuclease of a class 2 CRISPR-Cas system. *Cell* **163**, 759–771 (2015). doi: [10.1016/j.cell.2015.09.038](https://doi.org/10.1016/j.cell.2015.09.038); pmid: [26422227](https://pubmed.ncbi.nlm.nih.gov/26422227/)
- S. Shmakov *et al.*, Discovery and functional characterization of diverse class 2 CRISPR-Cas systems. *Mol. Cell* **60**, 385–397 (2015). doi: [10.1016/j.molcel.2015.10.008](https://doi.org/10.1016/j.molcel.2015.10.008); pmid: [26593719](https://pubmed.ncbi.nlm.nih.gov/26593719/)
- C. R. Hale *et al.*, Essential features and rational design of CRISPR RNAs that function with the Cas RAMP module complex to cleave RNAs. *Mol. Cell* **45**, 292–302 (2012). doi: [10.1016/j.molcel.2011.10.023](https://doi.org/10.1016/j.molcel.2011.10.023); pmid: [22277116](https://pubmed.ncbi.nlm.nih.gov/22277116/)
- W. Jiang, P. Samai, L. A. Marraffini, Degradation of phage transcripts by CRISPR-associated RNases enables type III CRISPR-Cas immunity. *Cell* **164**, 710–721 (2016). doi: [10.1016/j.cell.2015.12.053](https://doi.org/10.1016/j.cell.2015.12.053); pmid: [26853474](https://pubmed.ncbi.nlm.nih.gov/26853474/)
- P. Samai *et al.*, Co-transcriptional DNA and RNA cleavage during type III CRISPR-Cas immunity. *Cell* **161**, 1164–1174 (2015). doi: [10.1016/j.cell.2015.04.027](https://doi.org/10.1016/j.cell.2015.04.027); pmid: [25959775](https://pubmed.ncbi.nlm.nih.gov/25959775/)
- R. H. Staals *et al.*, Structure and activity of the RNA-targeting type III-B CRISPR-Cas complex of *Thermus thermophilus*. *Mol. Cell* **52**, 135–145 (2013). doi: [10.1016/j.molcel.2013.09.013](https://doi.org/10.1016/j.molcel.2013.09.013); pmid: [24119403](https://pubmed.ncbi.nlm.nih.gov/24119403/)
- R. H. Staals *et al.*, RNA targeting by the type III-A CRISPR-Cas Csm complex of *Thermus thermophilus*. *Mol. Cell* **56**, 518–530 (2014). doi: [10.1016/j.molcel.2014.10.005](https://doi.org/10.1016/j.molcel.2014.10.005); pmid: [25457165](https://pubmed.ncbi.nlm.nih.gov/25457165/)
- G. Tamulaitis *et al.*, Programmable RNA shredding by the type III-A CRISPR-Cas system of *Streptococcus thermophilus*. *Mol. Cell* **56**, 506–517 (2014). doi: [10.1016/j.molcel.2014.09.027](https://doi.org/10.1016/j.molcel.2014.09.027); pmid: [25458845](https://pubmed.ncbi.nlm.nih.gov/25458845/)
- V. Anantharaman, K. S. Makarova, A. M. Burroughs, E. V. Koonin, L. Aravind, Comprehensive analysis of the HEPN superfamily: Identification of novel roles in intra-genomic conflicts, defense, pathogenesis and RNA processing. *Biol. Direct* **8**, 15 (2013). doi: [10.1186/1745-6150-8-15](https://doi.org/10.1186/1745-6150-8-15); pmid: [23768067](https://pubmed.ncbi.nlm.nih.gov/23768067/)
- O. Niewoehner, M. Jinek, Structural basis for the endoribonuclease activity of the type III-A CRISPR-associated protein Csm6. *RNA* **22**, 318–329 (2016). doi: [10.1261/rna.054098.115](https://doi.org/10.1261/rna.054098.115); pmid: [26763118](https://pubmed.ncbi.nlm.nih.gov/26763118/)
- N. F. Sheppard, C. V. Glover 3rd, R. M. Terns, M. P. Terns, The CRISPR-associated Csx1 protein of *Pyrococcus furiosus* is an adenosine-specific endoribonuclease. *RNA* **22**, 216–224 (2016). doi: [10.1261/rna.039842.113](https://doi.org/10.1261/rna.039842.113); pmid: [26647461](https://pubmed.ncbi.nlm.nih.gov/26647461/)
- G. W. Goldberg, W. Jiang, D. Bikard, L. A. Marraffini, Conditional tolerance of temperate phages via transcription-dependent CRISPR-Cas targeting. *Nature* **514**, 633–637 (2014). doi: [10.1038/nature13637](https://doi.org/10.1038/nature13637); pmid: [25174707](https://pubmed.ncbi.nlm.nih.gov/25174707/)
- L. Deng, R. A. Garrett, S. A. Shah, X. Peng, Q. She, A novel interference mechanism by a type IIIB CRISPR-Cmr module in *Sulfolobus*. *Mol. Microbiol.* **87**, 1088–1099 (2013). doi: [10.1111/mmi.12152](https://doi.org/10.1111/mmi.12152); pmid: [23320564](https://pubmed.ncbi.nlm.nih.gov/23320564/)
- Y. K. Kim, Y. G. Kim, B. H. Oh, Crystal structure and nucleic acid-binding activity of the CRISPR-associated protein Csx1 of *Pyrococcus furiosus*. *Proteins* **81**, 261–270 (2013). doi: [10.1002/prot.24183](https://doi.org/10.1002/prot.24183); pmid: [22987782](https://pubmed.ncbi.nlm.nih.gov/22987782/)
- J. K. Nuñez, A. S. Lee, A. Engelman, J. A. Doudna, Integrase-mediated spacer acquisition during CRISPR-Cas adaptive immunity. *Nature* **519**, 193–198 (2015). doi: [10.1038/nature14237](https://doi.org/10.1038/nature14237); pmid: [25707795](https://pubmed.ncbi.nlm.nih.gov/25707795/)
- R. Heler *et al.*, Cas9 specifies functional viral targets during CRISPR-Cas adaptation. *Nature* **519**, 199–202 (2015). doi: [10.1038/nature14245](https://doi.org/10.1038/nature14245); pmid: [25707807](https://pubmed.ncbi.nlm.nih.gov/25707807/)
- J. K. Nuñez *et al.*, Cas1-Cas2 complex formation mediates spacer acquisition during CRISPR-Cas adaptive immunity. *Nat. Struct. Mol. Biol.* **21**, 528–534 (2014). doi: [10.1038/nsmb.2820](https://doi.org/10.1038/nsmb.2820); pmid: [24793649](https://pubmed.ncbi.nlm.nih.gov/24793649/)
- C. Díez-Villaseñor, N. M. Guzmán, C. Almendros, J. García-Martínez, F. J. Mojica, CRISPR-spacer integration reporter plasmids reveal distinct genuine acquisition specificities among CRISPR-Cas I-E variants of *Escherichia coli*. *RNA Biol.* **10**, 792–802 (2013). doi: [10.4161/rna.24023](https://doi.org/10.4161/rna.24023); pmid: [23445770](https://pubmed.ncbi.nlm.nih.gov/23445770/)
- I. Yosef, M. G. Goren, U. Qimron, Proteins and DNA elements essential for the CRISPR adaptation process in *Escherichia coli*. *Nucleic Acids Res.* **40**, 5569–5576 (2012). doi: [10.1093/nar/gks216](https://doi.org/10.1093/nar/gks216); pmid: [22402487](https://pubmed.ncbi.nlm.nih.gov/22402487/)
- K. A. Datsenko *et al.*, Molecular memory of prior infections activates the CRISPR/Cas adaptive bacterial immunity system. *Nat. Commun.* **3**, 945 (2012). doi: [10.1038/ncomms1937](https://doi.org/10.1038/ncomms1937); pmid: [22781758](https://pubmed.ncbi.nlm.nih.gov/22781758/)
- L. A. Marraffini, E. J. Sontheimer, Self versus non-self discrimination during CRISPR RNA-directed immunity. *Nature* **463**, 568–571 (2010). doi: [10.1038/nature08703](https://doi.org/10.1038/nature08703); pmid: [20072129](https://pubmed.ncbi.nlm.nih.gov/20072129/)
- C. R. Hale, A. Cocozaki, H. Li, R. M. Terns, M. P. Terns, Target RNA capture and cleavage by the Cmr type III-B CRISPR-Cas effector complex. *Genes Dev.* **28**, 2432–2443 (2014). doi: [10.1101/gad.250712.114](https://doi.org/10.1101/gad.250712.114); pmid: [25367038](https://pubmed.ncbi.nlm.nih.gov/25367038/)
- J. Zhang *et al.*, Structure and mechanism of the CMR complex for CRISPR-mediated antiviral immunity. *Mol. Cell* **45**, 303–313 (2012). doi: [10.1016/j.molcel.2011.12.013](https://doi.org/10.1016/j.molcel.2011.12.013); pmid: [22277115](https://pubmed.ncbi.nlm.nih.gov/22277115/)
- G. Kozlov *et al.*, Structural basis of defects in the saccin HEPN domain responsible for autosomal recessive spastic ataxia of Charlevoix-Saguenay (ARSACS). *J. Biol. Chem.* **286**, 20407–20412 (2011). doi: [10.1074/jbc.M11232884](https://doi.org/10.1074/jbc.M11232884); pmid: [21507954](https://pubmed.ncbi.nlm.nih.gov/21507954/)
- S. Kiani *et al.*, Cas9 gRNA engineering for genome editing, activation and repression. *Nat. Methods* **12**, 1051–1054 (2015). doi: [10.1038/nmeth.3580](https://doi.org/10.1038/nmeth.3580); pmid: [26344044](https://pubmed.ncbi.nlm.nih.gov/26344044/)
- S. Koneermann *et al.*, Genome-scale transcriptional activation by an engineered CRISPR-Cas9 complex. *Nature* **517**, 583–588 (2015). doi: [10.1038/nature14136](https://doi.org/10.1038/nature14136); pmid: [25494202](https://pubmed.ncbi.nlm.nih.gov/25494202/)
- J. E. Dahlman *et al.*, Orthogonal gene knockout and activation with a catalytically active Cas9 nuclease. *Nat. Biotechnol.* **33**, 1159–1161 (2015). doi: [10.1038/nbt.3390](https://doi.org/10.1038/nbt.3390); pmid: [26436575](https://pubmed.ncbi.nlm.nih.gov/26436575/)
- K. S. Makarova, Y. I. Wolf, E. V. Koonin, Comprehensive comparative-genomic analysis of type 2 toxin-antitoxin systems and related mobile stress response systems in prokaryotes. *Biol. Direct* **4**, 19 (2009). doi: [10.1186/1745-6150-4-19](https://doi.org/10.1186/1745-6150-4-19); pmid: [19493340](https://pubmed.ncbi.nlm.nih.gov/19493340/)
- F. Hayes, L. Van Melden, Toxins-antitoxins: Diversity, evolution and function. *Crit. Rev. Biochem. Mol. Biol.* **46**, 386–408 (2011). doi: [10.3109/10409238.2011.600437](https://doi.org/10.3109/10409238.2011.600437); pmid: [21819231](https://pubmed.ncbi.nlm.nih.gov/21819231/)
- K. S. Makarova, V. Anantharaman, L. Aravind, E. V. Koonin, Live virus-free or die: Coupling of antiviral immunity and programmed suicide or dormancy in prokaryotes. *Biol. Direct* **7**, 40 (2012). doi: [10.1186/1745-6150-7-40](https://doi.org/10.1186/1745-6150-7-40); pmid: [23151069](https://pubmed.ncbi.nlm.nih.gov/23151069/)
- C. Benda *et al.*, Structural model of a CRISPR RNA-silencing complex reveals the RNA-target cleavage activity in Cmr4. *Mol. Cell* **56**, 43–54 (2014). doi: [10.1016/j.molcel.2014.09.002](https://doi.org/10.1016/j.molcel.2014.09.002); pmid: [25280103](https://pubmed.ncbi.nlm.nih.gov/25280103/)
- Z. Abil, H. Zhao, Engineering reprogrammable RNA-binding proteins for study and manipulation of the transcriptome. *Mol. Biosyst.* **11**, 2658–2665 (2015). doi: [10.1039/C5MB00289C](https://doi.org/10.1039/C5MB00289C); pmid: [26166256](https://pubmed.ncbi.nlm.nih.gov/26166256/)
- J. P. Mackay, J. Font, D. J. Segal, The prospects for designer single-stranded RNA-binding proteins. *Nat. Struct. Mol. Biol.* **18**, 256–261 (2011). doi: [10.1038/nsmb.2005](https://doi.org/10.1038/nsmb.2005); pmid: [21358629](https://pubmed.ncbi.nlm.nih.gov/21358629/)

ACKNOWLEDGMENTS

We thank P. Boutz, J. Doench, P. Sharp, and B. Zetsche for helpful discussions and insights; R. Belliveau for overall research support; J. Francis and D. O'Connell for generous MiSeq instrument access; D. Daniels and C. Garvie for providing bacterial incubation space for protein purification; R. Macrae for critical reading of the manuscript; and the entire Zhang laboratory for support and advice. We thank N. Ranu for generously providing plasmid pRFZ and D. Daniels for providing 6-His-MBP-TEV. O.O.A. is supported by a Paul and Daisy Soros Fellowship, a Friends of the McGovern Institute Fellowship, and the Poitras Center for Affective Disorders. J.S.G. is supported by a U.S. Department of Energy (DOE) Computational Science Graduate Fellowship. S.S. is supported by the graduate program of Skoltech Data-Intensive Biomedicine and Biotechnology Center for Research, Education, and Innovation. I.M.S. is supported by the Simons Center for the Social Brain. D.B.T.C. is supported by award T32GM007753 from the National Institute of General Medical Sciences. K.S.M., E.V.K., and, in part, S.S. are supported by the intramural program of the U.S. Department of Health and Human Services (to the National Library of Medicine). K.S. is supported by NIH grant GM10407, Russian Science Foundation grant 14-14-00988, and Skoltech. F.Z. is a New York Stem Cell Foundation Robertson Investigator. F.Z. is supported by the NIH through the National Institute of Mental Health (5DP1-MH100706 and 1R01-MH110049), NSF, the New York Stem Cell, Simons, Paul G. Allen Family, and Vallee Foundations; and J. Poitras, P. Poitras, R. Metcalfe, and D. Cheng. A.R. is a member of the scientific advisory board for Syros Pharmaceuticals and Thermo Fisher. O.O.A., J.S.G., J.J., E.V.K., S.K., E.S.L., K.S.M., L.M., E.S., K.S., S.S., and F.Z. are inventors on provisional patent application 62/181,675 applied for by the Broad Institute, MIT, Harvard, NIH, Skoltech, and Rutgers that covers the C2c2 proteins described in this paper. Deep sequencing data are available at Sequence Read Archive under BioProject accession no. PRJNA318890. The authors plan to make the reagents widely available to the academic community through Addgene subject to a materials transfer agreement and to provide software tools via the Zhang laboratory website (www.genome-engineering.org) and GitHub (<https://github.com/fengzhanglab>).

SUPPLEMENTARY MATERIALS

www.sciencemag.org/content/353/6299/aaf5573/suppl/DC1
Materials and Methods
Tables S1 to S5
Figs. S1 to S24
References (51–55)

2 March 2016; accepted 25 May 2016
Published online 2 June 2016
10.1126/science.aaf5573

C2c2 is a single-component programmable RNA-guided RNA-targeting CRISPR effector

Omar O. Abudayyeh, Jonathan S. Gootenberg, Silvana Konermann, Julia Joung, Ian M. Slaymaker, David B. T. Cox, Sergey Shmakov, Kira S. Makarova, Ekaterina Semenova, Leonid Minakhin, Konstantin Severinov, Aviv Regev, Eric S. Lander, Eugene V. Koonin and Feng Zhang

Science **353** (6299), aaf5573.

DOI: 10.1126/science.aaf5573 originally published online June 2, 2016

ARTICLE TOOLS

<http://science.sciencemag.org/content/353/6299/aaf5573>

SUPPLEMENTARY MATERIALS

<http://science.sciencemag.org/content/suppl/2016/06/01/science.aaf5573.DC1>

RELATED CONTENT

<http://science.sciencemag.org/content/sci/353/6299/aad5147.full>

REFERENCES

This article cites 55 articles, 14 of which you can access for free
<http://science.sciencemag.org/content/353/6299/aaf5573#BIBL>

PERMISSIONS

<http://www.sciencemag.org/help/reprints-and-permissions>

Use of this article is subject to the [Terms of Service](#)